



Thermal and mechanical properties of mortar incorporated with paraffin/palm oil fuel ash composite



Sih Ying Kong^a, Ziu Hoe See^a, Chern Leing Lee^a, Xu Yang^{b,*}, Leong Sing Wong^c, Teck Shang Goh^d

^a School of Engineering, Monash University Malaysia, Bandar Sunway, 47500, Malaysia

^b Department of Civil Engineering, Monash University, Clayton, Victoria, 3800, Australia

^c Department of Civil Engineering, Universiti Tenaga Nasional, Kajang, 43000, Malaysia

^d WCT Construction Sdn Bhd, Petaling Jaya, 47301, Malaysia

ARTICLE INFO

Keywords:

Phase change materials
Palm oil fuel ash: POFA
Latent heat
Thermal properties

ABSTRACT

The aim of this research was to develop a form-stable phase change material by incorporating paraffin (PA) into palm oil fuel ash (POFA) through direct impregnation. The developed composite was characterized using Scanning electron microscope (SEM) and Fourier transform infrared spectroscopy (FTIR) to determine the microstructure and chemical property. The thermal properties of the composite was determined using Differential scanning calorimetry (DSC). The thermal reliability and thermal stability were assessed using Thermogravimetric analyser (TGA) and thermal cycling tests. Then, the developed form-stable composite was incorporated into cement mortar to evaluate their effects on compressive strength and thermal energy storage ability. From SEM results, PA was absorbed into pores of POFA. FTIR results showed there was no chemical interaction between PA and POFA. Latent heat of the composite was 13.34 J/g and 13.19 J/g for melting and solidification respectively. TGA and thermal cycling tests have validated that the composite was thermally stable and reliable. Incorporation of PA-POFA composite into cement mortar reduced compressive strength significantly. Incorporation of sufficient quantity of PA-POFA composite into cement mortar could increase thermal inertia and minimize temperature fluctuations of the mortar and model test room.

1. Introduction

Electric energy consumption by air conditioners and electric fan account for 20% of the total building energy consumption [1]. Due to the ever-growing population, there is a high demand for housing and commercial space globally which results in a persistent rise in buildings over the years, translating to increasing energy demand. Incorporation of phase change materials (PCMs) into building materials could potentially reduce the dependency of HVAC systems by acting as a latent heat thermal energy storage (LHTES) medium. It absorbs and releases substantial amounts of thermal energy from the environment during phase transition and when incorporated into building materials, could introduce thermal regulating properties.

PCMs are incorporated into building materials through direct incorporation, immersion and encapsulation techniques. Direct incorporation means PCMs are directly mixed with cementitious building materials during fabrication. For immersion technique, building

materials are submerged into liquid PCMs and absorbed through capillary action. Encapsulation is achieved by encapsulating PCMs within a suitable shell material. Encapsulated phase change materials are prepared in two methods, macroencapsulation and microencapsulation [2].

Form stable PCMs are prepared by impregnating PCMs into porous supporting materials by immersion or vacuum impregnation. Various porous medium such as diatomite [3–6], expanded perlite [4,7], expanded graphite [9–11], expanded vermiculite [12,8,13], pumice [14], molecular sieve [15], silica fume [16,17], cenosphere [18] and kaolin [19–21], have been used to prepare form-stable PCM. A research showed that paraffin impregnated lightweight aggregates could be used to produce lightweight concrete with a density of about 1700 kg/m³ and compressive strength up to 30 MPa [22]. A further research showed that lightweight concrete with compressive strength up to 53 MPa could be produced using mix design developed using Taguchi method [23].

The use of waste materials to produce form stable PCMs has been reported. The waste materials investigated are blast furnace slag [24,

* Corresponding author. Department of Civil Engineering, Monash University, Clayton, Victoria, 3800, Australia.

E-mail address: xu.yang@monash.edu (X. Yang).

25], waste glass powder [24]), carbonized abandoned rice [13,26], silicagel industrial wastes [27] and carbonized sunflower straw [28]. Palm oil fuel ash (POFA) is a waste material produced in immense amounts in Malaysia. The ash is derived from residues of palm oil industry waste burnt at a temperature range of 800 °C–1000 °C for electricity generation. POFA has been identified as a porous material with high silica content and it has been used as partial replacement of ordinary Portland cement to enhance the durability and strength of concrete [29–32].

POFA is a viable alternative to produce form-stable PCM composite due to its porous microstructure and easy availability in Malaysia. There is no study on characterization of thermal energy storage properties of PA-POFA composite and its application for cement mortar. Thermal energy storage mortar could be used as plaster coating of internal or external walls where it could reduce indoor temperature by absorbing heat energy thus reducing energy consumption for cooling. This research aims to evaluate chemical compatibility, thermal stability and latent heat of the proposed PA-POFA composite through SEM, FT-IR, TGA, DSC and thermal cycling tests. Then, effects of PA-POFA composite on compressive strength and heat storage capability of cement mortar were studied.

2. Experiment program

2.1. a. Materials

Organic phase change material, paraffin was chosen in this study due to its desirable properties such as high latent heat, thermally reliable during phase change process, non-corrosive and chemically inert. RT31 technical grade paraffin (PA) produced by Rubitherm with solid to liquid phase change temperatures of 27 °C–33 °C was utilized for this study. From the data sheet of RT31, the thermal conductivity is 0.2 W/mK, while the specific heat and heat capacity is 2 J/kgK and 165 kJ/kg, respectively. POFA was chosen as the medium to absorb PA as it has porous microstructure and available abundantly in Malaysia. POFA was obtained from Banting Palm Oil Mill, located in Selangor, Malaysia. The ash was derived from residues of palm oil industry waste burned at a temperature range of 800 °C–1000 °C for electricity generation. POFA was dried in an oven at 105 °C for 24 h to remove moisture and then sieved through a 425 µm sieve. Fig. 1 shows the sieved POFA used in this study. The chemical composition of POFA was determined using XRF machine (µEDX-1400 Shimadzu) at University Malaya and the results are listed in Table 1. The specific gravity of POFA was measured using pycnometer, while the BET specific surface area was obtained using gas absorption method (Micromeritics ASAP 2020). The median particle size of POFA was determined using Malvern Mastersizer 3000 series. The physical properties are listed in Table 1.

2.2. b. Preparation of form-stable PA-POFA composite

PA-POFA composite was prepared through direct impregnation technique by mixing PA and POFA at various mass ratios. Direct



Fig. 1. Sieved POFA.

Table 1

Chemical compositions and physical properties of POFA.

Chemical compositions	
Silicon dioxide (SiO ₂)	63.26%
Potassium oxide (K ₂ O)	17.52%
Calcium oxide (CaO)	13.63%
Iron oxide (Fe ₂ O ₃)	4.10%
Physical properties	
Specific surface area	9.8 m ² /g
Median particle size, d ₅₀	25.5 µm
Specific gravity	1.74 g/cm ³

impregnation was chosen over vacuum impregnation as it was reported that the difference between two methods was negligible [6]. The PA was heated above the melting temperature using a hot plate and it was in liquid form during preparation process. POFA was added into liquid PA and stirred constantly. The composite was then cooled down to room temperature where PA changed to solid state and form-stable PA-POFA composite was formed.

PA and POFA with mass ratios of 1:2, 1:3, 1:4, 1:5 and 1:6 were prepared and tested using the diffusion oozing circle test. The test was conducted by placing PA-POFA composite on filter papers within a marked circle of 30 mm diameter and then heated in an oven at 40 °C for 1 h. The mass ratio of 1:5 presented the highest absorption ratio with minimal leakage therefore it was chosen for the subsequent characterization and testing with cement mortar. Leakage percentage can be calculated through Eq (1) [7].

$$L\% = \frac{D_1 - D_0}{D_0} \times 100 \quad (1)$$

where D_0 is the diameter of test area (30 mm); D_1 is the diameter of PCM leakage.

2.3. c. Characterization of form stable PA-POFA composite

The morphology and microstructure of POFA and the developed form-stable PA-POFA composite was analysed using Hitachi SU8010 scanning electron microscope (SEM). The SEM was operated in the secondary electron detection mode with an accelerating voltage of 5 kV. The sample was sputter coated with platinum and placed on the carbon tape attached to the sample holder. The chemical compatibility between PA and POFA was investigated using a FTIR spectrophotometer from 400 cm⁻¹ to 4000 cm⁻¹. The FTIR analysis was performed using Thermo Scientific Nicolet iS10 via attenuated total reflectance method.

DSC tests were conducted to assess the phase change temperatures and latent heat of the prepared form stable PA-POFA composite. It was performed using PerkinElmer DSC 4000 and two-point calibration was done using indium and zinc. Around 10 mg sample was inserted into the sealed aluminium sample pan. The DSC tests were conducted from 10 °C to 50 °C at a scanning rate of 5 °C/min. TGA analysis was performed to evaluate the thermal stability of the composite using TA Instruments Q50 thermal gravimetric analyser. The analysis was carried out at a heating rate of 10 °C/min from room temperature to 600 °C. Nitrogen was used as the purge gas.

Thermal cyclic test was performed to evaluate the thermal reliability of PA-POFA composite after subjected to 1000 heating and cooling cycles. This was done using Bio-Rad T100 Thermal Cycler at Genomics Laboratory, Monash University Malaysia. The sample was heated to 70 °C and then cooled to 5 °C for 1000 cycles. DSC and FTIR tests were performed on the treated samples.

2.4. d. Compressive strength and thermal testing on mortar incorporated with PA-POFA composite

PA-POFA composite was integrated into cement mortar to produce thermal energy storage mortar (TESM). Four mix proportions were

considered as shown in Table 2, the control mortar without PA-POFA composite and mortar incorporated with 10%, 20% and 40% of PA-POFA composite by total volume. The composite was incorporated as a partial replacement of sand. The water-cement ratio and sand-cement ratio used for all mix designs was 0.65 and 2.75 respectively. The specific gravity for cement was 3.15, 2.7 for sand and 1.49 for the PA-POFA composite. Mortar cubes of $50 \times 50 \times 50 \text{ mm}^3$ were prepared for compressive strength tests. Two samples were prepared for each mix proportion. The samples were cured in a water bath at the room temperature for 28 days.

For thermal testing, mortar panels with dimensions of $200 \times 200 \times 50 \text{ mm}^3$ were fabricated for each mix proportion. The test setup consisted of a model room, a hot plate and thermocouples connected to a data logger. The model room was assembled using five polystyrene boards with a thickness of 25 mm and one mortar panel to form an enclosed space as shown in Fig. 2. Polystyrene boards were placed around the perimeter of the mortar panel to prevent heat loss to the surroundings. The model room was placed on top of a hot plate where the mortar panel was subjected to a constant temperature of 40°C for 6 hours and then cooled naturally for another 6 hours. Four thermocouples were placed on the inner surface of the mortar panel and one thermocouple at the centre of the model room to monitor temperature change.

3. Experimental results

Characterization results of PA-POFA composite were first presented to understand physical and chemical interactions between PA and POFA followed by thermal stability and heat capacity of PA-POFA composite. Then effects of PA-POFA composite on compressive strength and thermal properties of mortar were reported.

3.1. a. Leakage test of PA-POFA composite

Table 3 presents the leakage percentage of PA-POFA composite determined using Eq (1). It was observed that the composite showed severe leakage of 53.3% at a ratio of 1:3 (PA:POFA) followed by moderate leakage of 22.5% for the ratio of 1:4. Based on these results, the composite with the ratios of 1:3 and 1:4 was classified as extremely unstable and unstable, respectively [7]. While the composite with ratios of 1:5 and 1:6 were classified as stable because the percentage of leakage was equal to or less than 10%. Trace of paraffin observed on filter papers for these two ratios could be due to PA coating on the surface of POFA particles while PA absorbed in the pores remained stable due to capillary action. The optimum mass ratio was determined to be 1:5 for PA:POFA used in this study as it contained the largest quantity of PA while conforming to the classification of form stable PCM [7]. The composite with PA:POFA ratio of 1:5 will be characterized further in subsequent sections.

3.2. b. Morphology of PA-POFA composite

Fig. 2 presents the morphologies of both POFA and PA-POFA composite. Fig. 3 (a) and (b) show that POFA consisted of a mix of spherical and angular particles with porous microstructures. From these SEM images, it was observed that pore sizes ranged between $0.4 \mu\text{m}$ and $4 \mu\text{m}$

which allowed the absorption of the liquid PA. From Fig. 3 (c) and (d), it could be observed that PA has coated the POFA surface. In spite of the vacuum environment in the chamber, PA was still attached to POFA due to surface tension forces and capillary action. Coalescence of POFA particles was observed as paraffin acted as binder.

3.3. c. FTIR analysis of PA-POFA composite

FTIR analysis was carried out to characterize the chemical structures of PA, POFA and PA-POFA composite. From Fig. 4, three characteristic absorption bands observed for POFA were 580 cm^{-1} , 788 cm^{-1} and 1008 cm^{-1} similar to results reported by Runyut et al. [33]. The vibration peaks at 788 cm^{-1} and 1008 cm^{-1} corresponded to symmetric stretching vibrations of Si–O–Si groups and asymmetric stretching vibration of Si–O–T (T=Si or Al) groups which indicated presence of quartz materials. Whereas, four main characteristic peaks were identified for PA at 721 cm^{-1} , 1467 cm^{-1} , 2849 cm^{-1} and 2916 cm^{-1} . The peaks at 721 cm^{-1} and 1467 cm^{-1} signified bending vibrations of C–H while 2849 cm^{-1} and 2916 cm^{-1} corresponded to the symmetrical stretching vibrations of C–H.

The FTIR spectra for the PA-POFA composite showed that all main characteristic bands of PA and POFA were detected where peaks at 580 cm^{-1} , 788 cm^{-1} and 1004 cm^{-1} attributed to POFA particles while peaks at 720 cm^{-1} , 1467 cm^{-1} , 2849 cm^{-1} and 2916 cm^{-1} were related to PA. The minor shifts observed in some peaks could be due to physical interactions between PA and POFA such as capillary and surface tension forces [24]. Furthermore, no new band was detected in the spectra of PA-POFA composite and it could be concluded that no chemical reaction occurred between the functional groups of PA and POFA. Therefore, the FTIR results demonstrated a good chemical compatibility between PA and POFA.

3.4. d. Thermal stability of PA-POFA composite

TGA analysis was conducted on the PA-POFA composite to investigate its thermal stability. TGA curves for PA and the PA-POFA composite are presented in Fig. 5. For PA, a one-step weight loss was observed between 150°C and 260°C which signified the thermal decomposition of PA. The starting decomposition temperature was close to the flash point of RT 31 of 157°C . For PA-POFA composite, a two-step weight loss was identified where a sharp weight loss occurred at the temperature range of $150\text{--}200^\circ\text{C}$ due to thermal decomposition of PA. The gradual weight loss from 200°C to 600°C could be due to decomposition of paraffin absorbed in the POFA pores. The total weight loss was about 12%. As the decomposition temperature of PA-POFA composite was significantly higher than the phase change temperature ($27^\circ\text{C}\text{--}33^\circ\text{C}$), it could be concluded that the developed PA-POFA composite demonstrated good thermal stability and hence, is suitable for building applications.

3.5. e. Thermal properties of PA-POFA composite

Thermal energy storage performance and phase change temperatures of PA-POFA composite were determined through DSC analyses. The DSC curves with key information such as peak temperatures, onset temperatures and latent heat for both PA and PA-POFA composite are

Table 2
Mix proportions of mortar.

Constituent	Control		TESM-10		TESM-20		TESM-40	
	Volume (m^3)	Mass (kg)						
Cement	0.16	504	0.16	504	0.16	504	0.16	504
Water	0.33	328	0.33	328	0.33	328	0.33	328
Sand	0.51	1386	0.41	1116	0.31	846	0.11	306
PA-POFA	0	0	0.1	149	0.2	298	0.4	596

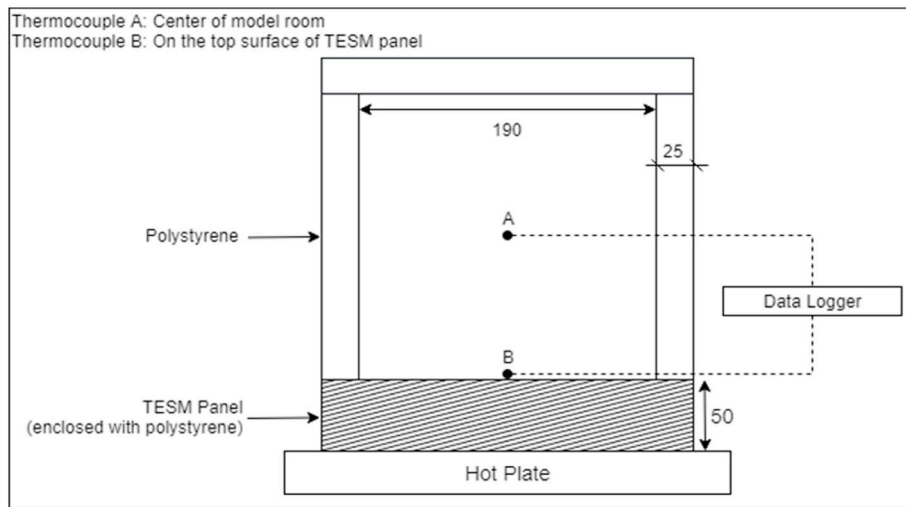
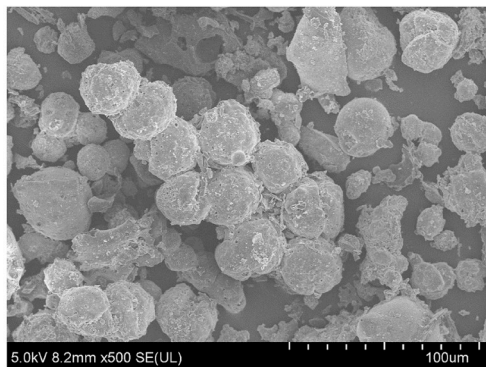


Fig. 2. Thermal testing on insulated mortar panels.

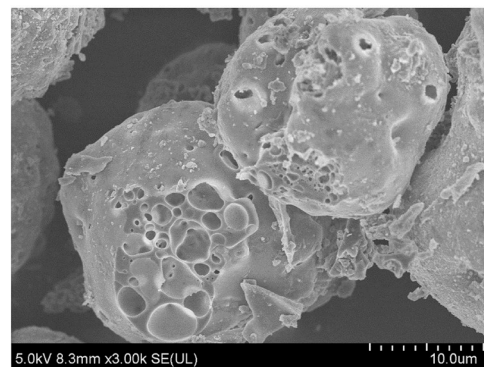
Table 3
Leakage test results.

PA:POFA proportion	1:3	1:4	1:5	1:6
Test diameter (mm)	30	30	30	30
Avg. diameter of leakage (mm)	46	36.75	33	32.75
Leakage percentage (%)	53.3	22.5	10	9.16

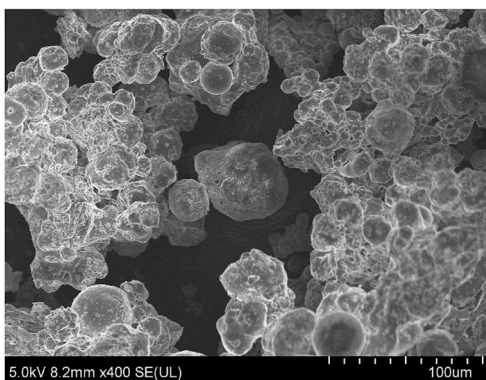
shown in Fig. 6. The onset temperature showed the melting or solidification temperature of a PCM. From Fig. 6, it could be observed that PA-POFA composite exhibited stable phase change behaviour. The melting and solidification temperatures for PA were 28.02 °C and 33.3 °C while they were 28.18 °C and 32.02 °C for PA-POFA composite. This showed that POFA reduced supercooling effect of PA, where the temperature difference between melting and solidification was 5.28 °C for PA, while it reduced to 3.84 °C for PA-POFA composite. The difference in melting and solidification temperatures between PA and PA-POFA composite were 0.16 °C and 1.28 °C respectively. The difference in the phase



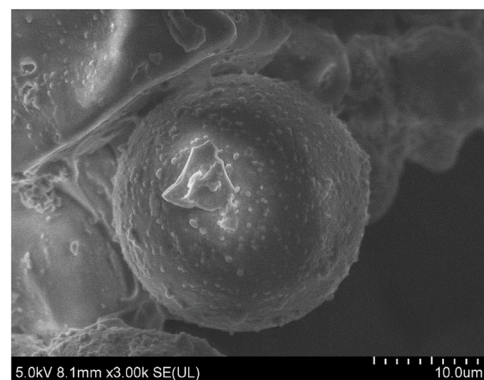
(a)



(b)



(c)



(d)

Fig. 3. SEM images of (a) POFA at 500× magnification; (b) POFA at 3000× magnification; (c) PA-POFA composite at 400× magnification; (d) PA-POFA composite at 3000× magnification.

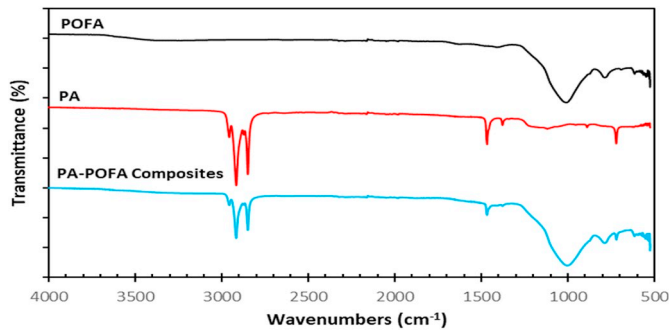


Fig. 4. FTIR spectrum for POFA, PA and PA-POFA composite.

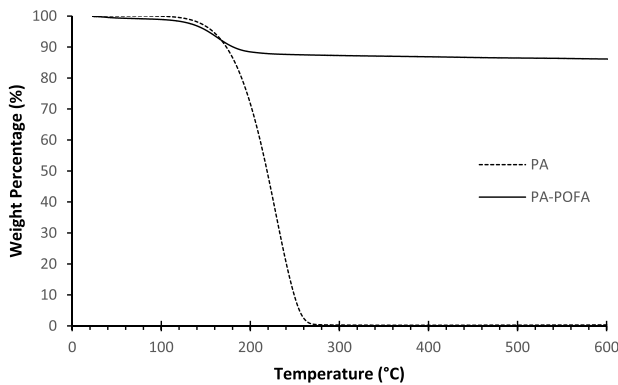


Fig. 5. TGA curves for PA and PA-POFA composite.

change temperatures could be attributed to the physical interaction between PA and POFA, thermal conductivity and pore structure of the POFA [34]. The latent heat for melting and solidification was identified to be 112.32 J/g and 114.45 J/g for PA. For PA-POFA composite, it was 13.34 J/g and 13.19 J/g, respectively. The weight percentage of PA impregnated into POFA could be calculated using Equation (2).

$$W\%_{PA} = \frac{\Delta H_{PA-POFA}}{\Delta H_{PA}} \times 100 \quad (2)$$

where $W\%_{PA}$ is the weight percentage of PA; ΔH_{PA} is the latent heat of PA; $\Delta H_{PA-POFA}$ is the latent heat of PA-POFA composite. The calculated weight percentage was 11.87% and it was consistent with the results from TGA analysis. The weight percentage of PA absorbed by POFA is comparable to octadecane absorbed by bentonite [35]. From these results, it could be deduced that the developed PA-POFA composite has suitable thermal energy storage potential for building application.

3.6. f. Long term stability of PA-POFA composite

PA-POFA composite was subjected to 1000 heating and cooling cycles and then the composite was tested using FTIR and DSC to evaluate its long term stability. From FTIR results, there was no change of peaks before and after 1000 cycles thus indicating that the chemical structure of PA-POFA composite was maintained. DSC curves for PA-POFA composite before and after thermal cyclic treatment are shown in Fig. 7. After the thermal cyclic treatment, the difference in phase change temperatures was determined to be 2.32 °C and 4.32 °C for melting and solidification, respectively. The latent heat reduced by about 10%, which was 1.28 J/g and 0.98 J/g for melting and solidification, respectively. The composite was considered as stable because the reduction in latent heat was minor and still acceptable for applications of thermal energy storage. However, the change of melting and solidify

temperatures over time could affect temperature regulation inside the buildings. Therefore more research is required to study the long term behaviour of PA-POFA composite.

3.7. g. Compressive strength of TESM

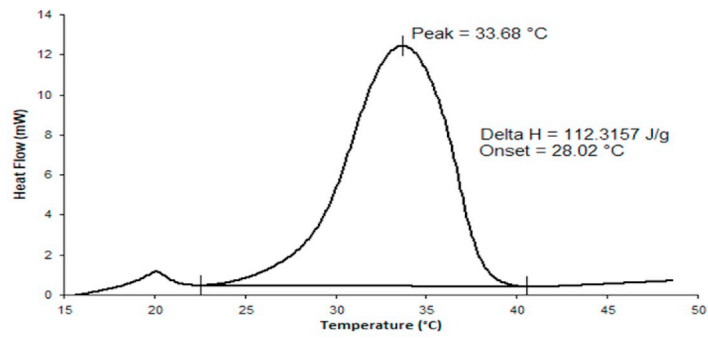
Fig. 8 presents the compressive strength of the control mortar and TESMs. It could be deduced from the results that increasing amounts of PA-POFA composite would reduce the compressive strength of mortar. The average compressive strength for the control, TESM 10, TESM 20 and TESM 40 was 26.4 MPa, 17.9 MPa, 12.7 MPa and 10.3 MPa, respectively. When the composite occupied 10%, 20% and 40% of the total volume, the percentage of reduction in compressive strengths was 32.2%, 52.1% and 61.2% respectively. The reduction of compressive strength could be attributed to unground POFA and PA used in this study.

POFA has been used to partially replace cement in concrete as it contributes to filler effect and pozzolanic reaction. POFA particles are finer than sand, they fill in the voids between sand and coarse aggregates thus producing a more homogeneous mix. POFA contains high percentage of silicon dioxide (SiO_2) and aluminium trioxide (Al_2O_3). Pozzolanic reaction occurs as SiO_2 and Al_2O_3 react with calcium hydroxide ($\text{Ca}(\text{OH})_2$) to form calcium silicate hydrate (C-S-H), calcium aluminate hydrate (C-A-H) and calcium silicate hydrate (C-A-S-H). It was found that ground POFA with smaller particle sizes than OPC could increase compressive strength of concrete when 20% of OPC Type I was replaced by ground POFA [36]. However, research also found that unground POFA was not a suitable pozzolanic material because it reduced the concrete compressive strength [29,37]. Noorvand et al. [29] also mentioned that addition of unground POFA weakened the microstructures of cement mortar due to the porous structure of POFA. Low pozzolanic reaction and porous microstructure of unground POFA caused reduction of mortar compressive strength in this study. Even though PA filled POFA voids in this study, PA has very low strength as it is in a gel form at the solid state, therefore it will not increase the strength of POFA. The reduction of compressive strength observed in this study could also be attributed to the PA adhered on the surface of POFA particles which hindered the pozzolanic reaction. PA adhered on the surface of POFA particles resulted in poor bonding at the interfacial transition zone (ITZ) and caused further reduction in compressive strength. Despite the significant loss in compressive strength, TESM-40 achieved more than 10 MPa which satisfied requirements for wall plastering applications and certain masonry mortar applications up to M10 mortar requirements based on BS EN 998-1 and BS EN 998-2.

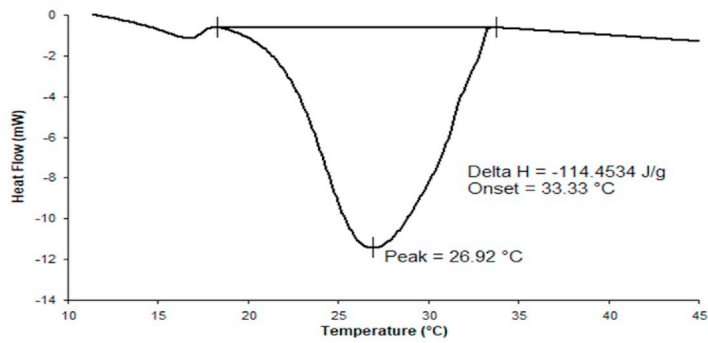
3.8. h. Thermal energy storage performance of TESM

Thermal energy storage performance of TESM was evaluated by monitoring the temperature change in the model test room and on the inner surface of the TESM when its outer surface was subjected to a constant temperature of 40 °C. The temperature time histories are presented in Fig. 9. Generally, a decreased rate of temperature rise was observed except TESM 10, and it became more prominent with increasing amounts of PA-POFA composite in mortar. These results showed that incorporation of 10% of PA-POFA composite in the mortar was not effective in increasing the heat absorption capacity of mortar. This could be attributed to the low quantity of PA added to mortar, where the added PA was about 2% only of the total mortar volume based on the chosen PA:POFA ratio of 1:5. Furthermore, TESM 10 showed a slightly higher rate of temperature gain at about 0.2 h compared to the control sample. This small variation could be due to the random errors as there was insufficient samples prepared for this test.

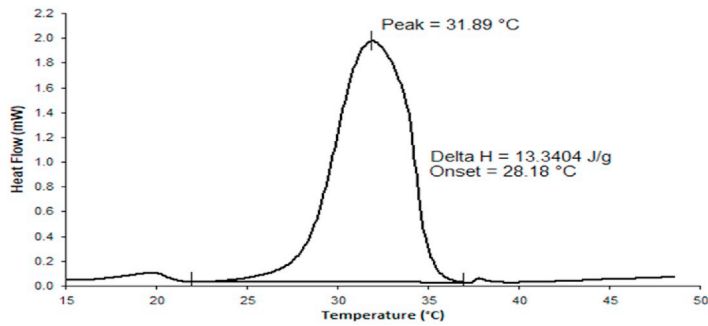
Thermal inertia of mortar could be improved by adding more than 20% of PA-POFA composite as the thermal lag effect could be observed clearly from TESM 20 and TESM 40 samples. For instance, TESM 20 and TESM 40 prolonged the time required for the inner surface to reach a



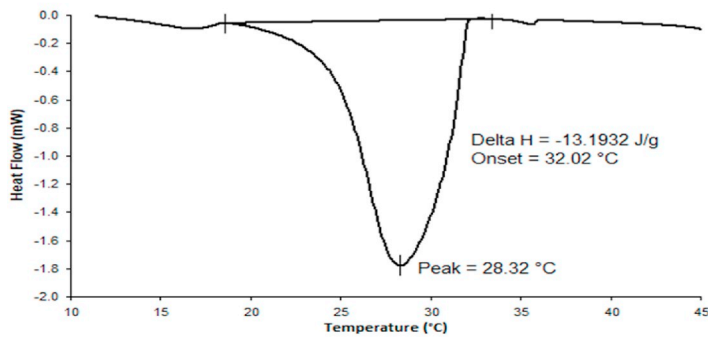
(a)



(b)



(c)



(d)

Fig. 6. DSC curves for (a) heating of PA; (b) cooling of PA; (c) heating of PA-POFA composite and (d) cooling of PA-POFA composite.

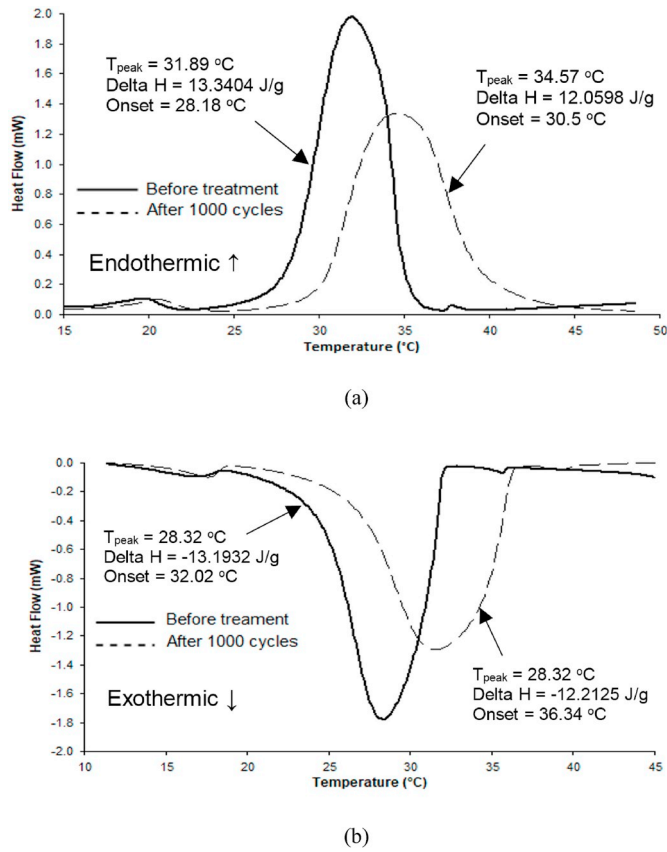


Fig. 7. DSC curves before and after 1000 thermal cycles: (a) heating; (b) cooling.

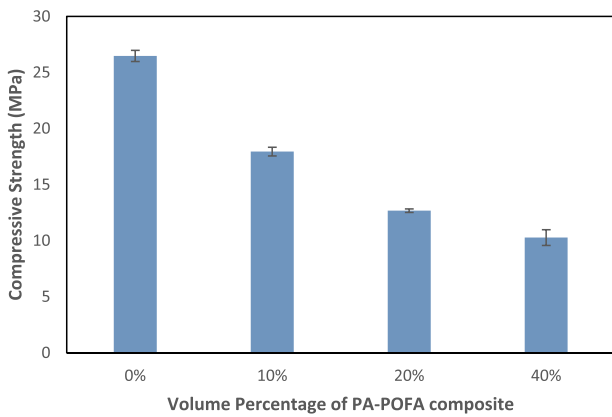


Fig. 8. Compressive strength of control and various TESM at 28 days.

temperature of $35\text{ }^{\circ}\text{C}$ by 27 and 68 min, respectively. The heat energy absorbed by PA during phase transition from solid state to liquid state contributed to the lower temperature increase rate observed. The maximum inner surface temperature of mortar panels observed was $39.1\text{ }^{\circ}\text{C}$, $38.8\text{ }^{\circ}\text{C}$, $38.3\text{ }^{\circ}\text{C}$ and $37.9\text{ }^{\circ}\text{C}$ for the control, TESM 10, TESM 20 and TESM 40, respectively. The maximum indoor temperature of the model test room was $35.6\text{ }^{\circ}\text{C}$, $35.4\text{ }^{\circ}\text{C}$, $35.2\text{ }^{\circ}\text{C}$ and $34.3\text{ }^{\circ}\text{C}$ for the control, TESM 10, TESM 20 and TESM 40, respectively. The temperature difference between the inner surfaces of the control mortar and TESM 40 sample was $1.2\text{ }^{\circ}\text{C}$ while it was $1.3\text{ }^{\circ}\text{C}$ for the indoor temperature between these two samples. These results demonstrated that the maximum temperatures of mortar panels and model test room reduced when

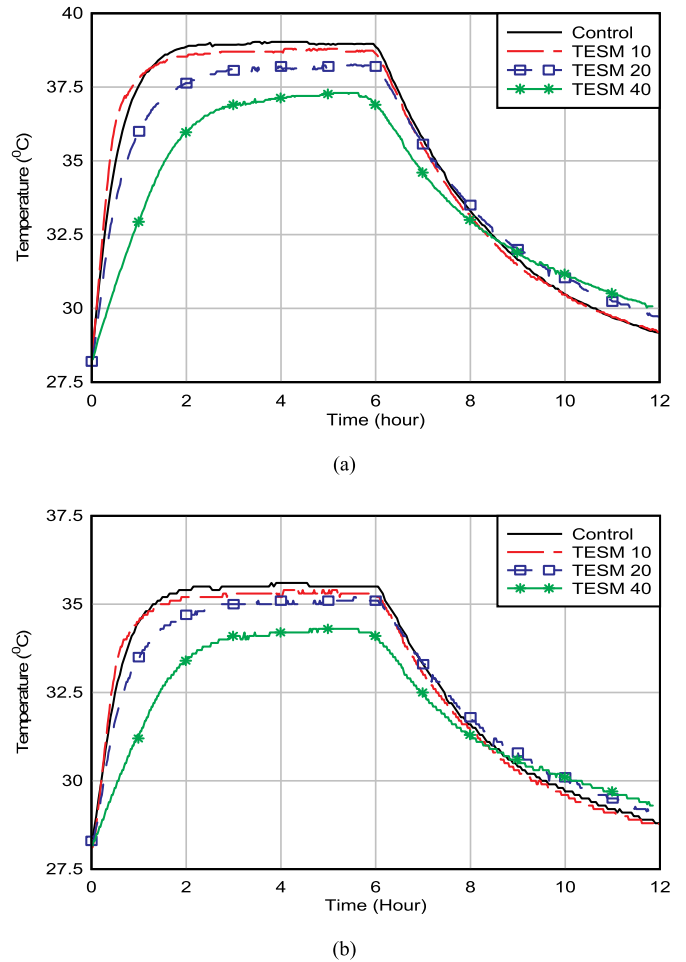


Fig. 9. Temperature time histories (a) on the inner surface of mortar panels; (b) at the middle of model room.

amounts of PA-POFA composite increased, even though the difference was not significant. The lower maximum temperature of TESM samples could be attributed to the low thermal conductivity of PA which is 0.2 W/mK . Fig. 9 depicts a reduced rate of heat loss for TESM 20 and TESM 40 compared to the control panel during the cooling phase. This phenomenon was caused by the discharge of thermal energy from PA when it changed from liquid state to solid state. This effect intensified with increasing amounts of PA-POFA composite.

Based on the results obtained, it could be deduced that by incorporating sufficient amount of PA-POFA composite into mortar, the thermal inertia of mortar increased and the temperature fluctuations in buildings could be reduced. It was worth noting that no leachate of PA could be observed from the samples after thermal testing which demonstrated short term stability of the mortar panels with PA-POFA composite. Further investigation on long term stability of mortar panels with PA-POFA composite is recommended.

4. Conclusion

This paper presented an experimental study to evaluate chemical and thermal properties of the proposed PA-POFA form stable PCM composite. Porous microstructures of POFA particles observed by the SEM analysis confirmed that POFA is a suitable medium to produce form stable phase change materials as PA could be confined successfully in POFA particles. The FTIR results showed that the PA and POFA were chemically compatible as there was no chemical reaction between PA and POFA that could affect the efficiency of PA to absorb heat energy.

TGA test results revealed that the decomposition temperature of PA-POFA composite was more than 100 °C, which was significantly higher than the phase change temperature of PA, therefore the PA-POFA composite could maintain good thermal stability within the normal buildings operating temperature range. The DSC analysis results showed that phase change temperatures of PA-POFA composite changed slightly compared to phase change temperatures of PA due to physical interaction between PA and POFA. The latent heat of PA-POFA composite was proportional to the amount of PA incorporated into POFA.

Incorporation of PA-POFA composite into cement mortar caused significant decrease in compressive strength due to lack of pozzolanic reaction and porous structures of unground POFA. The lower compressive strength could also be attributed to coating of PA on POFA particles surface which inhibited pozzolanic reaction and caused poor bonding at the interface transition zone. The results showed that cement mortar incorporated with 40% PA-POFA composite could achieve a compressive strength of 10 MPa, and it is suitable for wall plastering applications. By incorporating sufficient amount of PA-POFA composite into mortar, the thermal inertia of mortar increased and the temperature fluctuations in buildings could be reduced. The maximum temperature of TSM samples was reduced due to the low thermal conductivity of PA. Further investigations on long-term thermal stability and inflammability of thermal energy storage mortar incorporated with PA-POFA composite are recommended.

Acknowledgement

This work was undertaken with funding from Ministry of Higher Education, Malaysia under Fundamental Research Grant Scheme (FRGS) grant scheme (Program code. FRGS/1/2015/TK10/MUSM/03/1).

Appendix A. Supplementary data

Supplementary data to this article can be found online at <https://doi.org/10.1016/j.job.2019.100923>.

References

- [1] I.E. Agency, The Future of Cooling Opportunities for Energy-Efficient Air Conditioning, International Energy Agency, 2018.
- [2] S.A. Memon, Phase change materials integrated in building walls: a state of the art review, *Renew. Sustain. Energy Rev.* 31 (2014) 870–906.
- [3] M. Li, H. Kao, Z. Wu, J. Tan, Study on preparation and thermal property of binary fatty acid and the binary fatty acids/diatomite composite phase change materials, *Appl. Energy* 88 (5) (2011) 1606–1612.
- [4] A. Sari, A. Karaipekli, Fatty acid esters-based composite phase change materials for thermal energy storage in buildings, *Appl. Therm. Eng.* 37 (2012) 208–216.
- [5] B. Xu, Z. Li, Paraffin/diatomite composite phase change material incorporated cement-based composite for thermal energy storage, *Appl. Energy* 105 (2013) 229–237.
- [6] X. Li, J.G. Sanjayan, J.L. Wilson, Fabrication and stability of form-stable diatomite/paraffin phase change material composites, *Energy Build.* 76 (2014) 284–294.
- [7] L. Jiesheng, Y. Yuanyan, H. Xiang, Research on the preparation and properties of lauric acid/expanded perlite phase change materials, *Energy Build.* 110 (2016) 108–111.
- [8] X. Zhang, Z. Yin, D. Meng, Z. Huang, R. Wen, Y. Huang, X. Min, Y. Liu, M. Fang, X. Wu, Shape-stabilized composite phase change materials with high thermal conductivity based on stearic acid and modified expanded vermiculite, *Renew. Energy* 112 (2017) 113–123.
- [9] W. Fu, T. Zou, X. Liang, S. Wang, X. Gao, Z. Zhang, Y. Fang, Thermal properties and thermal conductivity enhancement of composite phase change material using sodium acetate trihydrate-urea/expanded graphite for radiant floor heating system, *Appl. Therm. Eng.* 138 (2018) 618–626.
- [10] X. Guo, S. Zhang, J. Cao, An energy-efficient composite by using expanded graphite stabilized paraffin as phase change material, *Compos. Appl. Sci. Manuf.* 107 (2018) 83–93.
- [11] Y. Yang, Y. Pang, Y. Liu, H. Guo, Preparation and thermal properties of polyethylene glycol/expanded graphite as novel form-stable phase change material for indoor energy saving, *Mater. Lett.* 216 (2018) 220–223.
- [12] X. Li, H. Wei, X. Lin, X. Xie, Preparation of stearic acid/modified expanded vermiculite composite phase change material with simultaneously enhanced thermal conductivity and latent heat, *Sol. Energy Mater. Sol. Cells* 155 (2016) 9–13.
- [13] X. Zhang, Z. Huang, Z. Yin, W. Zhang, Y. Huang, Y. Liu, M. Fang, X. Wu, X. Min, Form stable composite phase change materials from palmitic-lauric acid eutectic mixture and carbonized abandoned rice: preparation, characterization, and thermal conductivity enhancement, *Energy Build.* 154 (2017) 46–54.
- [14] A. Karaipekli, A. Sari, Development and thermal performance of pumice/organic PCM/gypsum composite plasters for thermal energy storage in buildings, *Sol. Energy Mater. Sol. Cells* 149 (2016) 19–28.
- [15] Z. Chen, F. Shan, L. Cao, G. Fang, Preparation and thermal properties of n-octadecane/molecular sieve composites as form-stable thermal energy storage materials for buildings, *Energy Build.* 49 (2012) 423–428.
- [16] Y. Wang, T.D. Xia, H. Zheng, H.X. Feng, Stearic acid/silica fume composite as form-stable phase change material for thermal energy storage, *Energy Build.* 43 (9) (2011) 2365–2370.
- [17] S.-G. Jeong, J. Jeon, J. Cha, J. Kim, S. Kim, Preparation and evaluation of thermal enhanced silica fume by incorporating organic PCM, for application to concrete, *Energy Build.* 62 (2013) 190–195.
- [18] F. Liu, J. Wang, X. Qian, Integrating phase change materials into concrete through microencapsulation using cenospheres, *Cement Concr. Compos.* 80 (2017) 317–325.
- [19] S. Ali Memon, T. Yiu Lo, X. Shi, S. Barbhuiya, H. Cui, Preparation, characterization and thermal properties of Lauryl alcohol/Kaolin as novel form-stable composite phase change material for thermal energy storage in buildings, *Appl. Therm. Eng.* 59 (1) (2013) 336–347.
- [20] A. Sari, Fabrication and thermal characterization of kaolin-based composite phase change materials for latent heat storage in buildings, *Energy Build.* 96 (2015) 193–200.
- [21] P. Lv, C. Liu, Z. Rao, Experiment study on the thermal properties of paraffin/kaolin thermal energy storage form-stable phase change materials, *Appl. Energy* 182 (2016) 475–487.
- [22] P. Sukontasukkul, E. Intawong, P. Preemano, P. Chindaprasit, Use of paraffin impregnated lightweight aggregates to improve thermal properties of concrete panels, *Mater. Struct.* 49 (5) (2016) 1793–1803.
- [23] P. Suttaphakdee, N. Dulsang, N. Lorwanishpaisarn, P. Kasemsiri, P. Posi, P. Chindaprasit, Optimizing mix proportion and properties of lightweight concrete incorporated phase change material paraffin/recycled concrete block composite, *Constr. Build. Mater.* 127 (2016) 475–483.
- [24] S.A. Memon, T.Y. Lo, H. Cui, Utilization of waste glass powder for latent heat storage application in buildings, *Energy Build.* 66 (2013) 405–414.
- [25] Y. Zhang, J. Liu, Z. Su, B. Liu, M. Lu, G. Li, C. Anderson, T. Jiang, Utilizing blast furnace slags (BFS) to prepare high-temperature composite phase change materials (C-PCMs), *Constr. Build. Mater.* 177 (2018) 184–191.
- [26] W. Gondora, K. Doudin, D.J. Nowakowski, B. Xiao, Y. Ding, T. Bridgwater, Q. Yuan, Encapsulation of phase change materials using rice-husk-char, *Appl. Energy* 182 (2016) 274–281.
- [27] K. Sun, Y. Kou, H. Zheng, X. Liu, Z. Tan, Q. Shi, Using silicage industrial wastes to synthesize polyethylene glycol/silica-hydroxyl form-stable phase change materials for thermal energy storage applications, *Sol. Energy Mater. Sol. Cells* 178 (2018) 139–145.
- [28] R. Wen, W. Zhang, Z. Lv, Z. Huang, W. Gao, A novel composite Phase change material of Stearic Acid/Carbonized sunflower straw for thermal energy storage, *Mater. Lett.* 215 (2018) 42–45.
- [29] H. Noorvand, A.A.A. Ali, R. Demirboga, H. Noorvand, N. Farzadnia, Physical and chemical characteristics of unground palm oil fuel ash cement mortars with nanosilica, *Constr. Build. Mater.* 48 (2013) 1104–1113.
- [30] M.M. Ul Islam, K.H. Mo, U.J. Alengaram, M.Z. Jumaat, Durability properties of sustainable concrete containing high volume palm oil waste materials, *J. Clean. Prod.* 137 (2016) 167–177.
- [31] B. Alsubari, P. Shafiqh, Z. Ibrahim, M.Z. Jumaat, Heat-treated palm oil fuel ash as an effective supplementary cementitious material originating from agriculture waste, *Constr. Build. Mater.* 167 (2018) 44–54.
- [32] H. Mohammadhosseini, M.M. Tahir, Durability performance of concrete incorporating waste metalized plastic fibres and palm oil fuel ash, *Constr. Build. Mater.* 180 (2018) 92–102.
- [33] D.A. Runyut, S. Robert, I. Ismail, R. Ahmadi, N.A. S.b.A. Samat, Microstructure and mechanical characterization of alkali-activated palm oil fuel ash, *J. Mater. Civ. Eng.* 30 (7) (2018), 04018119.
- [34] A. Sari, Thermal energy storage properties and laboratory-scale thermoregulation performance of bentonite/paraffin composite phase change material for energy-efficient buildings, *J. Mater. Civ. Eng.* 29 (6) (2017), 04017001.
- [35] Sar, Latent heat energy storage characteristics of building composites of bentonite clay and pumice sand with different organic PCMs, *Int. J. Energy Res.* 38 (11) (2014) 1478–1491.
- [36] P. Chindaprasit, T. Sinsiri, W. Kroehong, C. Jaturapitakkul, Role of filler effect and pozzolanic reaction of biomass ashes on hydrated phase and pore size distribution of blended cement paste, *J. Mater. Civ. Eng.* 26 (9) (2014), 04014057.
- [37] W. Tangchirapat, C. Jaturapitakkul, K. Kiattikomol, Compressive strength and expansion of blended cement mortar containing palm oil fuel ash, *J. Mater. Civ. Eng.* 21 (8) (2009) 426–431.